An International Journal of Optimization and Control: Theories & Applications
ISSN: 2146-0957 eISSN: 2146-5703
Vol.X, No.X, pp.X-X (2026)
https://doi.org/10.36922/IJOCTA026330207

RESEARCH ARTICLE

A dynamic study of cooperative hunting and a protected zone prey–predator model

Mustafa M. Subhi and Raid K. Naji*

Department of Mathematics, College of Science, University of Baghdad, Baghdad, Iraq
Mostafa.Sobhi2503p@sc.uobaghdad.edu.iq; raid.naji@sc.uobaghdad.edu.iq

ARTICLE INFO

Article history:
Received: August 11, 2026
Revised: September 25, 2026
Accepted: September 28, 2026
Published online: November 3, 2026

Keywords:
Protected and unprotected zones
Cooperative hunting
Stability
Bifurcation
Persistence

AMS Classification 2010: 34D20, 34C23

ABSTRACT

Predator–prey interactions are influenced by various ecological factors, including cooperative hunting, prey refuges, and harvesting, which can shape population dynamics, ecosystem stability, and species survival. This study proposes and studies a prey–predator system that interacts in two zones: the protected and the unprotected. It is assumed that the predator has the capability of cooperative hunting behavior. The objective of this study is to understand the role of a predator's capabilities in the dynamical behavior of the system. All the solution properties are studied. The stability analyses of the equilibria are investigated. The impact of perturbing the parameters is assessed using local bifurcation analysis. Persistence conditions of the system are established. Numerical simulations using the fourth-order Runge-Kutta method in MATLAB confirm all analytical results. It was shown that the system has at most two boundary equilibrium points, and the positive equilibrium point, if it exists, is multiple. In addition, a numerical study shows that the system with only point attractors exhibits a wide range of bistability behaviors.

CC BY

1. Introduction

Lotka-Volterra systems, first developed by Lotka[1] in 1925 and Volterra[2] in 1926, have grown in popularity over the past century in biomathematics and other ecological domains. In fact, researchers initially used them to investigate the dynamic behavior of distinct predator-prey systems that account for interactions among different species in an ecosystem. Later, researchers modeled other phenomena, including chemical processes,[3] hydrodynamics,[4] and plasma physics,[5] using a generic version of Lotka-Volterra systems. Many academics have recently presented their studies as predator-prey models in relation to many impacts, including the Allee effect,[6-8] immigration,[9-11] hunting cooperation,[12-14] the impact of fear,[15-17] cannibalism,[18-20] competition,[21] disease,[22-24] and more.

Predator hunting cooperation is one of the most significant effects in mathematical modeling. When predators hunt in groups, they can defeat prey that is too big, too swift, or too deadly for a single predator. At low predator densities, this creates positive density dependence: the kill rate doubles as the number of hunters doubles. Crucially, this can reverse the system. The cooperative group becomes the main factor influencing prey mortality rather than predators, which frequently results in sharp boom-and-bust cycles. However, that effect was independently suggested by several studies[25-27] that examined their influence on the dynamics of the prey-predator model, while other studies that examined hunting cooperation in relation to the fear effect were grounded in ecological data.[28-30] For example, wolves hunt in packs to encircle and pursue elk, frightening them not only because of the unexpected threat but also because they must remain vigilant and avoid areas where wolves are present.[31]

*Corresponding Author

The behavior of dynamics in prey-predator models with a reserved zone or refuge of prey to protect special biological species from extinction due to various external ecological forces and economic components, such as overpredation or harvesting, overexploitation, mismanagement of habitat, and pollution, has received a lot of attention in recent years in mathematical modeling of biology. As a result, several studies have examined this subject. For example, Dubey[32] created and examined a mathematical prey-predator model with a reserved zone and two distinct functional responses based on the predator's eating strategy. To determine the best harvesting benefits with acceptable taxes without pushing the ecosystem toward exploitation, Huo *et al.*[33] worked with a dynamic response model of a fisheries resource system in an aquatic setting. Naji and Jawad[34,35] presented a modified stage-structured predator-prey model with partially dependent predator and prey conservation after demonstrating the behavior and function of a reserve zone in a prey-predator system depending on the predator's eating mode. Murthy and Bahlool[36] studied the dynamics of the predator-prey model, in which the predator is assumed to be somewhat dependent on the prey for its growth, and the interaction between the species is governed by the Beddington-DeAngelis functional response. To explore the dynamics of an interaction between two species in which the predator can target both protected and unprotected regions, and to assess harvesting efforts on both species in both areas, Agnihotri and Nayyer[37] focused on a prey-predator model. The implications of toxicity and competition on the dynamics of the predator-prey model with a reserved zone were discussed by Louartassi *et al.*[38] Additionally, Rhiati *et al.*[39] analyzed the dynamics of an ecosystem model with a single predator and two comparable prey species interacting in a maritime environment with both protected and free regions. They also discussed the impact of applied harvesting effort in both zones.

Protected areas are designated geographic spaces where nature is managed for its long-term conservation, such as national parks, nature reserves, and marine sanctuaries. They are a key pillar in maintaining ecological stability and preventing species extinction worldwide. Keeping all the above in view, several governments around the world have taken serious measures to protect special biological species by decreasing the interactions of these species with external forces, such as restrictions on harvesting, and establishing many safe refuges for them, like Mudumalai National Park and Wildlife Sanctuary in India, England's marine conservation zones, and the United States' national wildlife refuge system. Building on this and the importance of cooperation in hunting as a key biological factor shaping prey-predator dynamics, we propose a new model that accounts for predator cooperation in hunting when prey move between protected and unprotected areas. This study aims to understand the role of predator potential in cooperation and its impact on dynamic behavior and survival in such an environment.

In this paper, the theoretical and applied aspects of our model are covered. In Section 2, the formulation of the model and the boundedness and positivity of solutions are presented. Additionally, the existence of equilibrium points and their local and global stability are investigated in Section 3. The local bifurcation and the persistence of the solutions of Equation 1 are discussed in Sections 4 and 5. The numerical simulation for our analytical results is presented in Section 6, and at the end of the paper, the conclusion is presented in Section 7.

2. The model formulation

A mathematical model was constructed to simulate the dynamics of an ecological system consisting of a prey species living in two zones (unprotected and protected) that interacts with a predator having a hunting cooperation property. It is assumed that the prey grows logistically in the absence of a predator, and it transfers between the two zones searching for food. The predator preys upon the prey in the unprotected zone, using its capability of cooperation in hunting and following a Lotka-Volterra type of functional response. However, it decays exponentially in the absence of the prey.

Let $x(t)$, $y(t)$, and $z(t)$ denote the populations of prey in the unprotected zone, protected zone, and a predator at time t. Then, the dynamics of the described prey-predator model can be written as **Equation 1**:

$$\begin{aligned}
\frac{dx}{dt} &= rx\left(1-\frac{x}{k}\right)-\sigma_1 x+\sigma_2 y-(\beta_1+\gamma z)xz \\
\frac{dy}{dt} &= sy\left(1-\frac{y}{l}\right)+\sigma_1 x-\sigma_2 y \\
\frac{dz}{dt} &= e(\beta_1+\gamma z)xz-\beta_0 z
\end{aligned} \tag{1}$$

where $x(t)\geq 0$, $y(t)\geq 0$, and $z(t)\geq 0$. All the parameters are assumed to be positive and are described in **Table 1**.

Table 1. Parameter description

Parameter	Description
σ_1	The prey's migration rate from unprotected to protected zones
σ_2	The prey's migration rate from protected to unprotected zones
r, s	The prey's growth rates for the unprotected and protected zones, respectively
k, l	The carrying capacities of unprotected and protected zones, respectively
β_0	The death rate coefficient of the predator species
β_1	The attack rate coefficient of the predator species
γ	The cooperative hunting coefficient
e	The conversion rate

Equation 1 has the following domain: $\mathcal{R}_+^3=\{(x,y,z): x(t)\geq 0, y(t)\geq 0, z(t)\geq 0\}$. Moreover, direct computation shows that all the partial derivatives of the right-hand side continuous functions of **Equation 1** are continuous. In addition, they are bounded as shown in Theorem 1. Therefore, the solution of **Equation 1** exists and is unique. Furthermore, according to **Equation 1**, it is easy to verify that:

- If there is no migration from protected to unprotected zones (i.e., $\sigma_2=0$) and $r-\sigma_1<0$, then $\frac{dx}{dt}<0$.
- If there is no migration from unprotected to protected zones (i.e., $\sigma_1=0$) and $s-\sigma_2<0$, then $\frac{dy}{dt}<0$.

Therefore, in our research, we always assumed that $\sigma_1>0$, $\sigma_2>0$, $r-\sigma_1>0$, and $s-\sigma_2>0$.

Theorem 1. All solutions of **Equation 1** that initiate in $\mathcal{R}_+^3$ are uniformly bounded.

Proof. Let $(x(t),y(t),z(t))$ be any solution of **Equation 1** with non-negative initial conditions $R(0)=(x(0),y(0),z(0))$, where $R(t)=x(t)+y(t)+z(t)$. Then, it is obtained that:

$$\frac{dR}{dt}=\frac{dx}{dt}+\frac{dy}{dt}+\frac{dz}{dt}\leq -\frac{r}{k}x^2+rx-\frac{s}{l}y^2+sy-\beta_0 z \quad (2)$$

Further simplification leads to **Equation 3**:

$$\frac{dR}{dt}+\zeta_0 R<-\frac{r}{k}x^2+2rx-\frac{s}{l}y^2+2sy < rk+sl=\mu_0 \quad (3)$$

where $\zeta_0=\min\{r,s,\beta_0\}$.

Thus, due to Lemma 2.1,[40] it is obtained that:

$$R(t)\leq \frac{\mu_0}{\zeta_0}\left[1-e^{-\zeta_0 t}\right]+R(0)e^{-\zeta_0 t} \quad (4)$$

Therefore, $0<R(t)\leq \frac{\mu_0}{\zeta_0}$ as $t\to\infty$. Hence, all solutions of **Equation 1** that initiate in $\mathcal{R}_+^3$ were confined in the following region (**Equation 5**):

$$\Omega=\left\{(x(t),y(t),z(t))\in\mathcal{R}_+^3: R(t)=x(t)+ y(t)+z(t)\leq \frac{\mu_0}{\zeta_0}\right\} \quad (5)$$

Thus, these solutions are uniformly bounded.

Theorem 2. For any $t>0$, all solutions of **Equation 1** with positive initial conditions are positive.

Proof. Assume that $\Gamma=\left\{\begin{matrix}(x(t),y(t),z(t))\in\mathcal{R}_+^3:\\ x(t)>0, y(t)>0, z(t)>0\end{matrix}\right\}$ represents the set of solutions with a positive initial point.

By using the initial condition $x(0)>0, y(0)>0, z(0)>0$ in the equations of **Equation 1**, and then integrating each one by dropping the main variable and solving the results as a separable equation, we get the following results:

$$x(t)=x(0)exp\left[\int_0^t\left[r\left(1-\frac{x(s)}{k}\right)-\sigma_1+\sigma_2\frac{y(s)}{x(s)}-(\beta_1+\gamma z(s))z(s)\right]ds\right]$$

$$y(t)=y(0)exp\left[\int_0^t\left[s\left(1-\frac{y(s)}{l}\right)+\sigma_1\frac{x(s)}{y(s)}-\sigma_2\right]ds\right]$$

$$z(t)=z(0)exp\left[\int_0^t\left[e(\beta_1+\gamma z(s))x(s)-\beta_0\right]ds\right] \quad (6)$$

The exponential function indicates that all solutions in Γ with positive initial conditions remain in the first octant. Hence, the proof is done.

3. The equilibria with their stability analysis

Understanding the "what-if" possibilities of our ecosystems is essentially the goal of studying the stability of equilibrium points in environmental mathematical models. Ecologists and mathematicians search for equilibrium points, states in which the system is perfectly balanced and nothing is changing, when creating models to depict populations and their interactions. On paper, however, a balance is meaningless if the slightest breeze overturns the entire system. Stability analysis can help with that.

Direct computation shows that **Equation 1** has at most three nonnegative equilibrium points, which can be described as:

(i) The trivial equilibrium point $(\mathcal{TEP})$, which is denoted by $E_0=(0,0,0)$, always exists.

(ii) The predator-free equilibrium point $(\mathcal{PTDFEP})$, which is denoted by $E_1=(\hat{x},y,0)$, is defined as:

$$\hat{y}=\frac{\hat{x}\left(rx-k\left(r-\sigma_1\right)\right)}{k\sigma_2} \tag{7}$$

where $\hat{x}$ represents the positive root of the equation:

$$\begin{aligned}&-sr^2x^3+2ksr\left(r-\sigma_1\right)x^2\\&+k\left[lr\sigma_2\left(s-\sigma_2\right)-s\left(r-\sigma_1\right)^2\right]x\\&-l\sigma_2k^2\left(rs-s\sigma_1-r\sigma_2\right)=0\end{aligned} \tag{8}$$

Consequently, using Descartes' rule of signs shows that $\mathcal{PDFEP}$ exists uniquely in the first quarter of the plane provided that the following conditions are met:

$$k\left(r-\sigma_1\right)<r\hat{x} \tag{9}$$

$$ks\left(r-\sigma_1\right)^2<lr\sigma_2\left(s-\sigma_2\right) \tag{10}$$

$$s\left(r-\sigma_1\right)<r\sigma_2 \tag{11}$$

(iii) The positive equilibrium point $(\mathcal{PSEP})$ is denoted by $E_2=(\tilde{x},\tilde{y},\tilde{z})$, where:

$$\tilde{x}=\frac{s\tilde{y}^2-l\tilde{y}\left(s-\sigma_2\right)}{l\sigma_1} \tag{12}$$

$$\tilde{z}=\frac{\beta_0-e\beta_1\tilde{x}}{e\gamma\tilde{x}}=\frac{-\beta_1+\dfrac{l\beta_0\sigma_1}{e\tilde{y}\left(s\tilde{y}-l\left(s-\sigma_2\right)\right)}}{\gamma} \tag{13}$$

while $\tilde{y}$ represents the positive root of the equation:

$$\begin{aligned}&h_6y^6+h_5y^5+h_4y^4+h_3y^3\\&+h_2y^2+h_1y+h_0=0\end{aligned} \tag{14}$$

where the coefficients are defined as:

$$h_6=-e^2rs^3\gamma,$$

$$h_5=3e^2lrs^2\gamma\left(s-\sigma_2\right),$$

$$h_4=sl\gamma e^2\left[ks\sigma_1\left(r-\sigma_1\right)-3rl\left(s-\sigma_2\right)^2\right],$$

$$h_3=\gamma e^2l^2\left[lr\left(s-\sigma_2\right)^3-2ks^2\sigma_1\left(r-\sigma_1\right)+ks\sigma_1\sigma_2\left(2r-\sigma_1\right)\right]$$

$$h_2=ekl^2\sigma_1\left[elr\gamma\left(s-\sigma_2\right)^2-s\sigma_1\left(els\gamma-\beta_0\beta_1-el\gamma\sigma_2\right)\right]$$

$$h_1=-ekl^3\beta_0\beta_1\sigma_1^2\left(s-\sigma_2\right),$$

$$h_0=-kl^3\beta_0^2\sigma_1^3.$$

Using Descartes' rule of signs shows that **Equation 14** has either zero positive roots or multiple positive roots. However, $\tilde{x}$ and $\tilde{z}$ are positive if the following conditions are met:

$$l\left(s-\sigma_2\right)<s\tilde{y} \tag{15}$$

$$\beta_1<\frac{\beta_0}{e\tilde{x}} \tag{16}$$

Now, the local behavior of **Equation 1** for each of the previous three equilibrium points will be studied. Firstly, the Jacobian matrix $(\mathcal{JM})$ of **Equation 1** at $\mathcal{TEP}$ can be determined as:

$$J\left(E_0\right)=\begin{bmatrix}r-\sigma_1 & \sigma_2 & 0\\ \sigma_1 & s-\sigma_2 & 0\\ 0 & 0 & -\beta_0\end{bmatrix} \tag{17}$$

Then, the characteristic polynomial $(\mathcal{CP})$ of $J\left(E_0\right)$ is given by:

$$\begin{aligned}&\left(-\beta_0-\lambda\right)\left[\lambda^2-\left(r-\sigma_1+s-\sigma_2\right)\lambda+\right.\\&\left.\left(\left(r-\sigma_1\right)\left(s-\sigma_2\right)-\sigma_1\sigma_2\right)\right]=0\end{aligned} \tag{18}$$

Accordingly,

$$\lambda_{01},\lambda_{02}=\frac{\left(r-\sigma_1+s-\sigma_2\right)}{2}\pm\frac{\sqrt{\left(r-\sigma_1+s-\sigma_2\right)^2-4\left(\left(r-\sigma_1\right)\left(s-\sigma_2\right)-\sigma_1\sigma_2\right)}}{2},$$

and $\lambda_{03}=-\beta_0$ represent the eigenvalues $(\mathcal{EVS})$ of

$J(E_0)$. Therefore, $\mathcal{TRFEP}$ becomes a saddle point due to $\lambda_{03}<0$ and $(r-\sigma_1+s-\sigma_2)>0$.

The $\mathcal{JM}$ at $\mathcal{PDFEP}$ can be written as **Equation 19**:

$$J(E_1)=\left[\hat{a}_{ij}\right]=\begin{bmatrix} -2\frac{r\hat{x}}{k}+r-\sigma_1 & \sigma_2 & -\beta_1\hat{x} \\ \sigma_1 & -2\frac{s\hat{y}}{l}+s-\sigma_2 & 0 \\ 0 & 0 & -\beta_0+e\beta_1\hat{x} \end{bmatrix} \tag{19}$$

Then, the $\mathcal{CP}$ of $J(E_1)$ is given by **Equation 20**:

$$\begin{aligned}&(e\beta_1\hat{x}-\beta_0-\lambda)\left[\lambda^2-(a_{11}+a_{22})\lambda+\right.\\&\left.(\hat{a}_{11}a_{22}-\hat{a}_{12}a_{21})\right]=0\end{aligned} \tag{20}$$

Accordingly,

$$\lambda_{11},\lambda_{12}=\frac{(\hat{a}_{11}+a_{22})\pm\sqrt{(a_{11}+\hat{a}_{22})^2-4(a_{11}\hat{a}_{22}-a_{12}a_{21})}}{2},$$

and $\lambda_{13}=e\beta_1\hat{x}-\beta_0$ represent the $\mathcal{EVS}$ of $J(E_1)$. Therefore, $\mathcal{PDFEP}$ becomes locally asymptotically stable ($\mathcal{LAS}$) if the following conditions are met:

$$e\beta_1\hat{x}<\beta_0 \tag{21}$$

$$\hat{a}_{11}<0 \tag{22}$$

$$\hat{a}_{22}<0 \tag{23}$$

$$\hat{a}_{11}a_{22}-a_{12}a_{21}>0 \tag{24}$$

The $\mathcal{JM}$ at $\mathcal{PSEP}$ can be written as:

$$J(E_2)=\left[\tilde{a}_{ij}\right]=\begin{bmatrix} \tilde{a}_{11} & \tilde{a}_{12} & \tilde{a}_{13} \\ \tilde{a}_{21} & \tilde{a}_{22} & 0 \\ \tilde{a}_{31} & 0 & \tilde{a}_{33} \end{bmatrix} \tag{25}$$

where:

$\tilde{a}_{11}=-2\frac{r\tilde{x}}{k}+r-\sigma_1-\tilde{z}(\gamma\tilde{z}+\beta_1)$, $\tilde{a}_{12}=\sigma_2$,

$\tilde{a}_{13}=-2\gamma\tilde{x}\tilde{z}-\beta_1\tilde{x}$, $\tilde{a}_{21}=\sigma_1$, $\tilde{a}_{22}=-2\frac{s\tilde{y}}{l}+s-\sigma_2$,

$\tilde{a}_{31}=e\tilde{z}(\gamma\tilde{z}+\beta_1)$ and $\tilde{a}_{33}=2e\gamma\tilde{x}\tilde{z}-\beta_0+e\tilde{x}\beta_1$, so the $\mathcal{CP}$ of $J(E_2)$ can be written as:

$$\lambda^3+A_1\lambda^2+A_2\lambda+A_3=0 \tag{26}$$

where:

$A_1=-(\tilde{a}_{11}+\tilde{a}_{22}+\tilde{a}_{33})$,

$A_2=\tilde{a}_{11}\tilde{a}_{22}-\tilde{a}_{12}\tilde{a}_{21}+\tilde{a}_{11}\tilde{a}_{33}-\tilde{a}_{13}\tilde{a}_{31}+\tilde{a}_{22}\tilde{a}_{33}$,

$A_3=-\tilde{a}_{33}(\tilde{a}_{11}\tilde{a}_{22}-\tilde{a}_{12}\tilde{a}_{21})+\tilde{a}_{13}\tilde{a}_{22}\tilde{a}_{31}$,

$$\begin{aligned}&A_1A_2-A_3=-(\tilde{a}_{11}+\tilde{a}_{22})(\tilde{a}_{11}\tilde{a}_{22}-\tilde{a}_{12}\tilde{a}_{21})\\&-(\tilde{a}_{11}+\tilde{a}_{33})(\tilde{a}_{11}\tilde{a}_{33}-\tilde{a}_{13}\tilde{a}_{31})\\&-\tilde{a}_{22}\tilde{a}_{33}(2\tilde{a}_{11}+\tilde{a}_{22}+\tilde{a}_{33})\end{aligned}$$

With $\tilde{a}_{ij}$ for all $i,j=1,2,3$ are the elements of $J(E_2)$.

According to the Routh-Hurwitz criterion, **Equation 26** has three $\mathcal{EVS}$ with negative real parts provided that the necessary and sufficient conditions $A_1>0$, $A_3>0$, and $A_1A_2-A_3>0$ are satisfied, and that can be done if the following conditions are satisfied:

$$(r-\sigma_1)<\frac{2r}{k}\tilde{x}+\beta_1\tilde{z}+\gamma\tilde{z}^2 \tag{27}$$

$$(s-\sigma_2)<\frac{2s}{l}\tilde{y} \tag{28}$$

$$e\beta_1\tilde{x}+2e\gamma\tilde{x}\tilde{z}<\beta_0 \tag{29}$$

$$\begin{aligned}\sigma_1\sigma_2<&\left(-\frac{2r}{k}\tilde{x}-\beta_1\tilde{z}-\gamma\tilde{z}^2+(r-\sigma_1)\right)\\&\left(-\frac{2s}{l}\tilde{y}+(s-\sigma_2)\right)\end{aligned} \tag{30}$$

Thus, **Equations 27–30** guarantee the $\mathcal{LAS}$ of $\mathcal{PSEP}$.

It is well known that an equilibrium point is globally asymptotically stable ($\mathcal{GAS}$) in the region $\mathcal{Q}$, which means that the long-time behavior of the system's solution starting from any initial point in the region $\mathcal{Q}$ will ultimately converge to the equilibrium point. Therefore, when there are multiple equilibrium points in the *int.* $\mathcal{R}_+^3$, the $\mathcal{GAS}$ will not be possible. Accordingly, in the following, we considered the $\mathcal{GAS}$ of the $\mathcal{PDFEP}$.

Theorem 3. The $\mathcal{PDFEP}$ is $\mathcal{GAS}$ in the region

$$\hat{\Gamma}=\left\{(x(t),y(t),z(t))\in\mathcal{R}_+^3:x(t)>0,y(t)>0,z(t)\geq 0\right\}$$

if the following condition holds:

$$\gamma\hat{x}\left(z_{max}+\frac{\beta_1}{\gamma}\right)<\frac{\beta_0}{e} \tag{31}$$

where z_{max} is the upper bound of the variable z that results from Theorem 1.

Proof. Consider the following positive definite candidate Lyapunov function on the region $\hat{\Gamma}$:

$$V(x,y,z)=c_1\left(x-\hat{x}-x\ln\frac{x}{\hat{x}}\right)+c_2\left(y-y-y\ln\frac{y}{y}\right)+c_3 z \tag{32}$$

where c_1, c_2, and c_3 are positive constants, then:

$$\begin{aligned}\frac{dV}{dt}&=c_1\left(\frac{x-\hat{x}}{x}\right)\left(-\frac{r}{k}x^2+(r-\sigma_1)x+\sigma_2 y-\beta_1 xz\right.\\&\left.-\gamma xz^2\right)+c_2\left(\frac{y-\hat{y}}{y}\right)\left(-\frac{s}{l}y^2+(s-\sigma_2)y+\sigma_1 x\right)\\&+c_3\left(e\beta_1 xz+e\gamma xz^2-\beta_0 z\right)\end{aligned} \tag{33}$$

By the use of some mathematical manipulation, it is obtained that:

$$\begin{aligned}\frac{dV}{dt}&=-c_1\frac{r}{k}(x-\hat{x})^2+c_1\frac{\sigma_2}{\hat{x}x}(x-x)(xy-xy)\\&-c_1\gamma(x-\hat{x})\left(z^2+\frac{\beta_1}{\gamma}z\right)-c_2\frac{s}{l}(y-y)^2+\\&c_2\frac{\sigma_1}{\hat{y}y}(y-\hat{y})(xy-xy)+c_3 e\gamma x\left(z^2+\frac{\beta_1}{\gamma}z\right)-c_3\beta_0 z\end{aligned} \tag{34}$$

Selecting the positive constants as $c_1=1$, $c_2=\frac{\sigma_2\hat{y}}{\sigma_1\hat{x}}$, and $c_3=\frac{1}{e}$, and substituting into the above equation yields:

$$\begin{aligned}\frac{dV}{dt}&=-\frac{r}{k}(x-\hat{x})^2+\frac{\sigma_2}{\hat{x}x}(x-x)(xy-xy)\\&-\gamma(x-\hat{x})\left(z^2+\frac{\beta_1}{\gamma}z\right)-\left(\frac{\sigma_2 s\hat{y}}{\sigma_1 l\hat{x}}\right)(y-y)^2\\&+\frac{\sigma_2}{\hat{x}y}(y-\hat{y})(xy-xy)+\gamma x\left(z^2+\frac{\beta_1}{\gamma}z\right)-\frac{\beta_0}{e}z\end{aligned} \tag{35}$$

Further simplification leads to:

$$\begin{aligned}\frac{dV}{dt}&=-\frac{r}{k}(x-\hat{x})^2-\left(\frac{\sigma_2 s\hat{y}}{\sigma_1 l\hat{x}}\right)(y-y)^2-\\&\left[\frac{\beta_0}{e}-\gamma\hat{x}\left(z+\frac{\beta_1}{\gamma}\right)\right]z-\frac{\sigma_2}{\hat{x}xy}(xy-xy)^2\end{aligned} \tag{36}$$

Thus, $\frac{dV}{dt}$ is negative definite under **Equation 31**. Therefore, due to the Lyapunov direct method, $\mathcal{PDFEP}$ is $\mathcal{GAS}$.

4. Local bifurcation

Local bifurcation is a qualitative shift in the local dynamics of an ecological system that happens when a biological parameter surpasses a particular threshold. Understanding, anticipating, and even controlling abrupt, severe changes in ecosystem status is the main goal of research on local bifurcation. It shifts ecology from a seamless transition to one that considers tipping points. Thus, the possibility of a local bifurcation in **Equation 1** is examined in this section.

Equation 1 can be rewritten in a vector form as:

$$\begin{aligned}&\frac{d\boldsymbol{X}}{dt}=\boldsymbol{F}(\boldsymbol{X},\mu)\ ,\ \boldsymbol{X}=(x,y,z)^T\\&\boldsymbol{F}(\boldsymbol{X},\mu)=\left(f_1(\boldsymbol{X},\mu),f_2(\boldsymbol{X},\mu),f_3(\boldsymbol{X},\mu)\right)^T\end{aligned} \tag{37}$$

where $f_i(x,y,z),\forall i=1,2,3$ are given by:

$$f_1(\boldsymbol{X},\mu)=-\frac{r}{k}x^2+(r-\sigma_1)x+\sigma_2 y-\beta_1 xz-\gamma xz^2,$$

$$f_2(\boldsymbol{X},\mu)=-\frac{s}{l}y^2+(s-\sigma_2)y+\sigma_1 x,$$

$$f_3(\boldsymbol{X},\mu)=e\beta_1 xz+e\gamma xz^2-\beta_0 z.$$

Moreover, $\mu\in\mathbb{R}_+$ is the possible bifurcation parameter to be determined.

Now, for any vector $V=(v_1,v_2,v_3)^T$, a direct calculation was made to obtain the second and third derivatives of vector **F**, as:

$$D^2\boldsymbol{F}(\boldsymbol{X},\mu)\cdot(V,V)=\begin{pmatrix}-2\gamma v_3^2 x-4\gamma v_1 v_3 z-\frac{2r}{k}v_1^2-2\beta_1 v_1 v_3\\-\frac{2s}{l}v_2^2\\2e\gamma v_3^2 x+4e\gamma v_1 v_3 z+2e\beta_1 v_1 v_3\end{pmatrix} \tag{38}$$

while:

$$D^3\boldsymbol{F}(\boldsymbol{X},\mu)\cdot(V,V,V)=\begin{pmatrix}-6\gamma v_1 v_3^2\\0\\6e\gamma v_1 v_3^2\end{pmatrix} \tag{39}$$

Theorem 4. When the parameter e crosses the value $\hat{e}=\frac{\beta_0}{\beta_1\hat{x}}$, **Equation 1** near $\mathcal{PDFEP}$ has a transcritical bifurcation ($\mathcal{TCB}$) if the following conditions hold:

$$\gamma\hat{x}+\beta_1 v_{11}\neq 0 \tag{40}$$

$$\hat{a}_{11}a_{22}-a_{12}a_{21}\neq 0 \tag{41}$$

It has a Pitchfork bifurcation ($\mathcal{PFB}$) when **Equation 40** is violated.

Proof. The $\mathcal{JM}$ at $\mathcal{PDFEP}$, which is given in **Equation 19**, at $\left(E_1,\hat{e}\right)$ transfers to the form:

$$\hat{J}=J\left(E_1,\hat{e}\right)=\begin{bmatrix}\hat{a}_{11} & a_{12} & a_{13}\\ a_{21} & \hat{a}_{22} & 0\\ 0 & 0 & 0\end{bmatrix}$$

Therefore, $\hat{J}$ has a zero $\mathcal{EVS}$ that is given by $\hat{\lambda}_{13}=0$. Assume that $V_1=\left(v_{11},v_{21},v_{31}\right)^T$ and $W_1=\left(w_{11},w_{21},w_{31}\right)^T$ are the eigenvectors of $\hat{J}$ and $\hat{J}^T$ corresponding to $\hat{\lambda}_{13}=0$, respectively. Straightforward computations lead to $V_1=\left(-\frac{\hat{a}_{13}a_{22}}{\hat{a}_{11}\hat{a}_{22}-a_{12}a_{21}},\frac{a_{13}a_{21}}{a_{11}a_{22}-a_{12}a_{21}},1\right)^T$ and $W_1=\left(0,0,1\right)^T$.

Moreover, according to Sotomayor's Theorem,[41] the following results are obtained:

$$\boldsymbol{F}_{\mathrm{e}}\left(\boldsymbol{X},e\right)=\frac{d\boldsymbol{F}\left(\boldsymbol{X},e\right)}{d\mathrm{e}}=\begin{pmatrix}0\\0\\\beta_1 xz+\gamma xz^2\end{pmatrix}\Rightarrow \boldsymbol{F}_e\left(E_1,\hat{e}\right)=\begin{pmatrix}0\\0\\0\end{pmatrix}$$

Consequently, it is obtained that $W_1^T\boldsymbol{F}_e\left(E_1,\hat{e}\right)=0$.

$$D\boldsymbol{F}_e\left(\boldsymbol{X},e\right)=\begin{bmatrix}0 & 0 & 0\\ 0 & 0 & 0\\ \beta_1 z+\gamma z^2 & 0 & \beta_1 x+2\gamma xz\end{bmatrix}\Rightarrow D\boldsymbol{F}_e\left(E_1,\hat{e}\right)\cdot V_1=\begin{pmatrix}0\\0\\\beta_1\hat{x}\end{pmatrix}$$

Consequently, it is obtained that

$$W_1^T D\boldsymbol{F}_e\left(E_1,\hat{e}\right)\cdot V_1=\beta_1\hat{x}\neq 0$$

Furthermore, by the use of **Equation 38**, it results in:

$$D^2\boldsymbol{F}\left(E_1,\hat{e}\right)\cdot\left(V_1,V_1\right)=\begin{pmatrix}-2\gamma\hat{x}-\frac{2r}{k}v_{11}^2-2\beta_1 v_{11}\\ -\frac{2s}{l}v_{21}^2\\ 2e\gamma\hat{x}+2e\beta_1 v_{11}\end{pmatrix}$$

Consequently, due to **Equations 40**–**41**, it is obtained that:

$$W_1^T D^2\boldsymbol{F}\left(E_1,\hat{e}\right)\cdot\left(V_1,V_1\right)=2e\gamma x+2e\beta_1 v_{11}\neq 0$$

Then, **Equation 1** near $\mathcal{PDFEP}$ has a $\mathcal{TCB}$.

When **Equation 40** is violated, then by the use of **Equation 39**, it results in:

$$D^3\boldsymbol{F}\left(E_1,\hat{e}\right)\cdot\left(V_1,V_1,V_1\right)=\begin{pmatrix}-6\gamma v_{11}\\ 0\\ 6e\gamma v_{11}\end{pmatrix}$$

Therefore, it is obtained that:

$$W_1^T D^3\boldsymbol{F}\left(E_1,\hat{e}\right)\cdot\left(V_1,V_1,V_1\right)=6e\gamma v_{11}\neq 0.$$

Then, **Equation 1**near $\mathcal{PDFEP}$ has a $\mathcal{PFB}$.

Theorem 5. When the parameter β_0 crosses the positive value $\tilde{\beta}_0=2e\gamma\tilde{x}\tilde{z}+e\tilde{x}\beta_1-\frac{\tilde{a}_{13}\tilde{a}_{22}\tilde{a}_{31}}{\left(\tilde{a}_{11}\tilde{a}_{22}-\tilde{a}_{12}\tilde{a}_{21}\right)}$, **Equation 1** near $\mathcal{PSEP}$ has a saddle-node bifurcation ($\mathcal{SNB}$) if the following conditions are held:

$$\begin{aligned}&w_{12}\left(-2\gamma\tilde{x}-4\gamma v_{12}\tilde{z}-\frac{2r}{k}v_{12}^2-2\beta_1 v_{12}\right)+w_{22}\\&\left(-\frac{2s}{l}v_{22}^2\right)+\left(2e\gamma\tilde{x}+4e\gamma v_{12}\tilde{z}+2e\beta_1 v_{12}\right)\neq 0\end{aligned} \tag{42}$$

$$\tilde{a}_{11}\tilde{a}_{22}-\tilde{a}_{12}\tilde{a}_{21}\neq 0 \tag{43}$$

Proof. The $\mathcal{JM}$ at $\mathcal{PSEP}$, which is given in **Equation 25**, at $\left(E_2,\tilde{\beta}_0\right)$ transfers to the form:

$$\tilde{J}=J\left(E_2,\tilde{\beta}_0\right)=\begin{bmatrix}\tilde{a}_{11} & \tilde{a}_{12} & \tilde{a}_{13}\\ \tilde{a}_{21} & \tilde{a}_{22} & 0\\ \tilde{a}_{31} & 0 & \tilde{a}_{33}^*\end{bmatrix}$$

where $\tilde{a}_{33}^*=\tilde{a}_{33}\left(\tilde{\beta}_0\right)=0$ and $\tilde{a}_{ij}$ for all $i,j=1,2,3$ are the elements of $J\left(E_2\right)$.

It is simple to prove that the determinant of $\tilde{J}$ at $\beta_0=\tilde{\beta}_0$ equals zero. Hence, the $\mathcal{CP}$ of $\tilde{J}$ has a zero $\mathcal{EV}$, say $\tilde{\lambda}_3=0$. Thus, $\mathcal{PSEP}$ becomes a non-hyperbolic point when $\beta_0=\tilde{\beta}_0$.

Now, assume that $V_2=\left(v_{12},v_{22},v_{32}\right)^T$ and $W_2=\left(w_{12},w_{22},w_{32}\right)^T$ are the eigenvectors of $\tilde{J}$ and $\tilde{J}^T$ corresponding to $\tilde{\lambda}_3=0$, respectively. Straightforward computations lead to $V_2=\left(-\frac{\tilde{a}_{13}\tilde{a}_{22}}{\tilde{a}_{11}\tilde{a}_{22}-\tilde{a}_{12}\tilde{a}_{21}},\frac{\tilde{a}_{13}\tilde{a}_{21}}{\tilde{a}_{11}\tilde{a}_{22}-\tilde{a}_{12}\tilde{a}_{21}},1\right)^T$ and $W_2=\left(-\frac{\tilde{a}_{22}\tilde{a}_{31}}{\tilde{a}_{11}\tilde{a}_{22}-\tilde{a}_{12}\tilde{a}_{21}},\frac{\tilde{a}_{12}\tilde{a}_{31}}{\tilde{a}_{11}\tilde{a}_{22}-\tilde{a}_{12}\tilde{a}_{21}},1\right)^T$.

Moreover, according to Sotomayor's Theorem[41] the following results are obtained:

$$\boldsymbol{F}_{\beta_0}(\boldsymbol{X},\beta_0)=\frac{d\boldsymbol{F}(\boldsymbol{X},\beta_0)}{d\beta_0}=\begin{pmatrix}0\\0\\-z\end{pmatrix}\Rightarrow \boldsymbol{F}_{\beta_0}\left(E_2,\tilde{\beta}_0\right)=\begin{pmatrix}0\\0\\-\tilde{z}\end{pmatrix}$$

Consequently, it is obtained that

$$W_2^T\boldsymbol{F}_{\beta_0}\left(E_2,\tilde{\beta}_0\right)=-\tilde{z}\neq 0$$

Furthermore, by the use of **Equation 38**, it results in:

$$D^2\boldsymbol{F}(E_2,\beta_0)\cdot(V_2,V_2)=\begin{pmatrix}-2\gamma\tilde{x}-4\gamma v_{12}\tilde{z}-\frac{2r}{k}v_{12}^2-2\beta_1 v_{12}\\-\frac{2s}{l}v_{22}^2\\2e\gamma\tilde{x}+4e\gamma v_{12}\tilde{z}+2e\beta_1 v_{12}\end{pmatrix}$$

Consequently, due to **Equations 42**–**43**, it is obtained that:

$$W_2^T D^2\boldsymbol{F}\left(E_2,\beta_0\right)\cdot\left(V_2,V_2\right)=w_{12}\left(-2\gamma\tilde{x}-4\gamma v_{12}\tilde{z}-\frac{2r}{k}v_{12}^2-2\beta_1 v_{12}\right)+w_{22}\left(-\frac{2s}{l}v_{22}^2\right)+\left(2e\gamma\tilde{x}+4e\gamma v_{12}\tilde{z}+2e\beta_1 v_{12}\right)\neq 0$$

Then, **Equation 1** near $\mathcal{PSEP}$ has a $\mathcal{SNB}$.

5. The persistence

Understanding the long-term survivability and stability of species, populations, or the system as a whole in the face of disruptions, changes in the environment, or internal dynamics is the goal of researching persistence in ecological systems. More precisely, researching persistence changes the focus of ecological inquiry from "Do species exist today?" to "Will they continue to exist for some time to come?" This change is crucial for both basic science and practical environmental decision-making.

In this section, the persistence of our biological system is presented, and this is done by showing that **Equation 1** has no omega limit set on the boundary planes.

Theorem 6. Assume that:

$$\beta_0<e\beta_1\hat{x} \tag{44}$$

Then, **Equation 1** is uniformly persistent if **Equation 44** holds.

Proof. Suppose that u is a point in the *Int.* $\mathcal{R}_+^3$ and $o(u)$ is the orbit through u. Let $\Omega(u)$ be the omega limit set of $o(u)$. Note that $\Omega(u)$ is bounded due to Theorem (1). Now, to show that $E_0\notin\Omega(u)$, assume the contrary.

Since E_0 is a saddle point, by the Butler-McGhie lemma,[42] E_0 cannot be the only point in $\Omega(u)$, and hence there is at least one other point v such that $v\in\omega^s(E_0)\cap\Omega(u)$, where $\omega^s(E_0)$ is the stable manifold of E_0.

Furthermore, since $\omega^s(E_0)$ is the positive $z-axis$ and the entire orbit through v, say $o(v)$, is contained in $\Omega(u)$. It follows that the positive specific axis (that contains v) is contained in $\Omega(u)$, which contradicts its boundedness. Thus, we obtain that $E_0\notin\Omega(u)$.

Now, to prove that $E_1\notin\Omega(u)$, we assume the contrary too. Since E_1 is a saddle point under **Equation 44**, then again by the Butler-McGhie lemma, there is another point $v_1\in\omega^s(E_1)\cap\Omega(u)$. Moreover, due to **Equations 22**–**24**, $\omega^s(E_1)$ is the first quadrant of the $xy-plane$, say $\mathcal{N}$.

Note that if v_1 is on either boundary axis of $\mathcal{N}$, then we get a contradiction as in the first part of the proof. Otherwise, in case v_1 belongs to the interior of $\mathcal{N}$, since E_1 is an equilibrium point in the interior of $\mathcal{N}$, then $o(v_1)$ either is unbounded, which gives a contradiction, or has a nonempty alpha limit set denoted by $\alpha(v_1)$, with $\alpha(v_1)=E_1$. Hence, we have a contradiction too, as an unstable point may not be in an omega limit set.

Therefore, it is obtained $E_1\notin\Omega(u)$. Thus $\Omega(u)$ must be in the *Int.* $\mathcal{R}_+^3(xyz)$, which guarantees the persistence of **Equation 1**.

6. Numerical simulation

The numerical solution of ecological systems complements the analytical solution obtained from the study of stability, persistence, and bifurcation. It confirms these results and shows how they are affected by slight changes in the parameter values. Thus, the numerical solution determines the set of parameters affecting the dynamics of the ecosystem. Therefore, the fourth-order Runge-Kutta method was utilized through MATLAB version R2021a code to solve **Equation 1** starting from 16 positive initial points and the following biologically feasible set of estimated parameter values.

$$\begin{aligned}&r=2,k=20,\sigma_1=0.4,\sigma_2=0.6,\beta_1=0.2\\&\gamma=0.15,s=1,l=10,\beta_0=0.1,e=0.2\end{aligned} \tag{45}$$

The obtained numerical solutions were presented in the form of a three-dimensional phase plot that explains the solutions of **Equation 1** in its domain and a two-dimensional long-term behavior plot of the solution versus time that explains the solutions in the direction of each variable as a function of time. All the initial points are represented in blue, while the final state equilibrium points are represented in red.

For **Equation 45** with different positive initial points, the solutions of **Equation 1** approached $E_1 = (1.72, 5.3, 0)$ and $E_2 = (0.45, 4.41, 5.92)$, which indicated a bistable behavior (**Figure 1**).

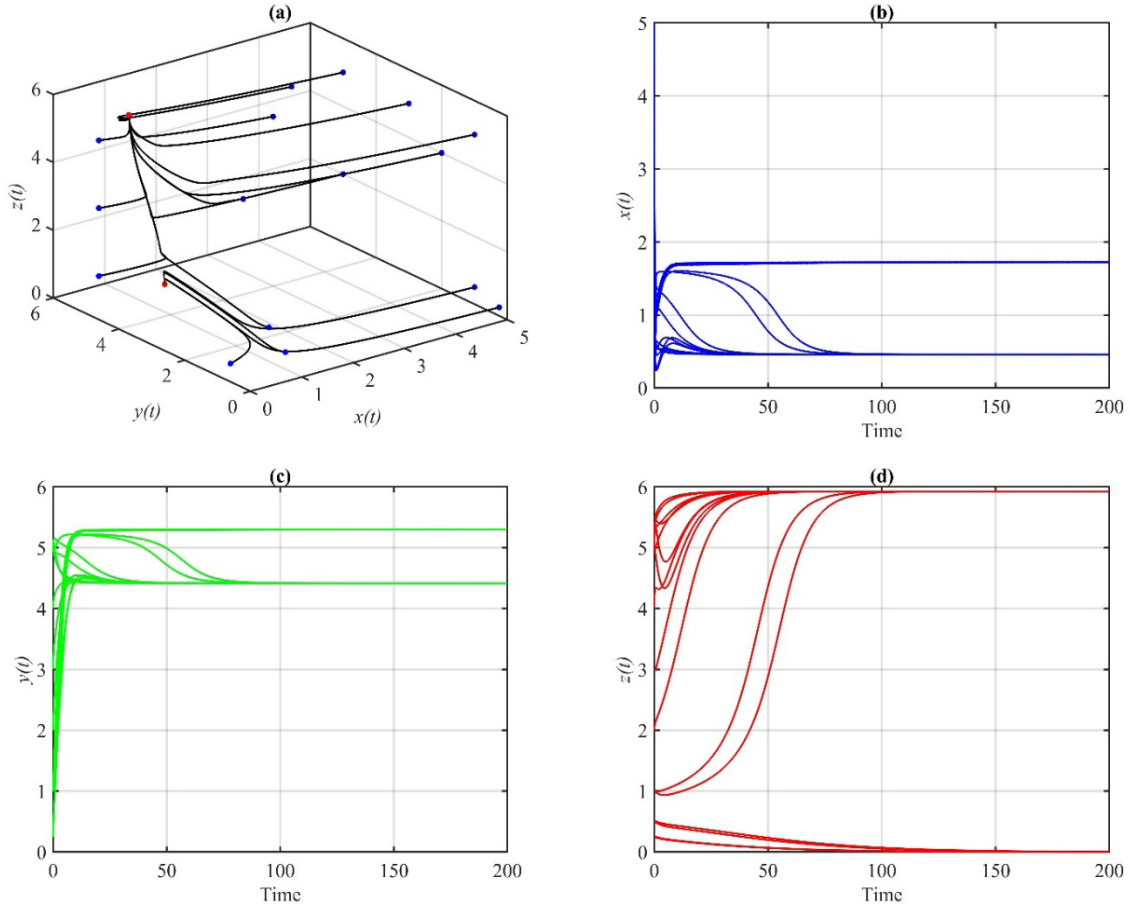


Figure 1. The numerical solutions of **Equation 1** utilizing **Equation 45** and various positive initial points. (a) Three-dimensional phase plot shows bistable behavior. (b) Two-dimensional (2D) long-term behavior of $x(t)$. (c) 2D long-term behavior of $y(t)$. (d) 2D long-term behavior of $z(t)$.

The absence of the positive point's global stability is depicted in **Figure 1**. Furthermore, it implies that under the same environmental circumstances, an ecosystem can live in two distinct stable states.

Altering the parameter r in the ranges $r < 0.94$ and $r \geq 0.94$ makes **Equation 1** approach E_2 and bistability between E_1 and E_2, respectively (**Figure 2**).

Figure 2 explains that when $r < 0.94$, E_1 disappears, and the system will approach E_2; otherwise, the system undergoes bistability behavior. This indicates that, for low values of the prey's growth rate in the unprotected zone, under the same environmental circumstances, an ecosystem can live at a positive stable state.

It is observed that varying the parameters k and σ_1, while keeping the other parameter values as in **Equation 45**, has a quantitative influence on the dynamical behavior of **Equation 1**. However, altering the parameter σ_2 in the ranges $\sigma_2 < 0.16$ and $\sigma_2 \geq 0.16$ makes **Equation 1** approach E_1 and bistability between E_1 and E_2, respectively (**Figures 1** and **3**).

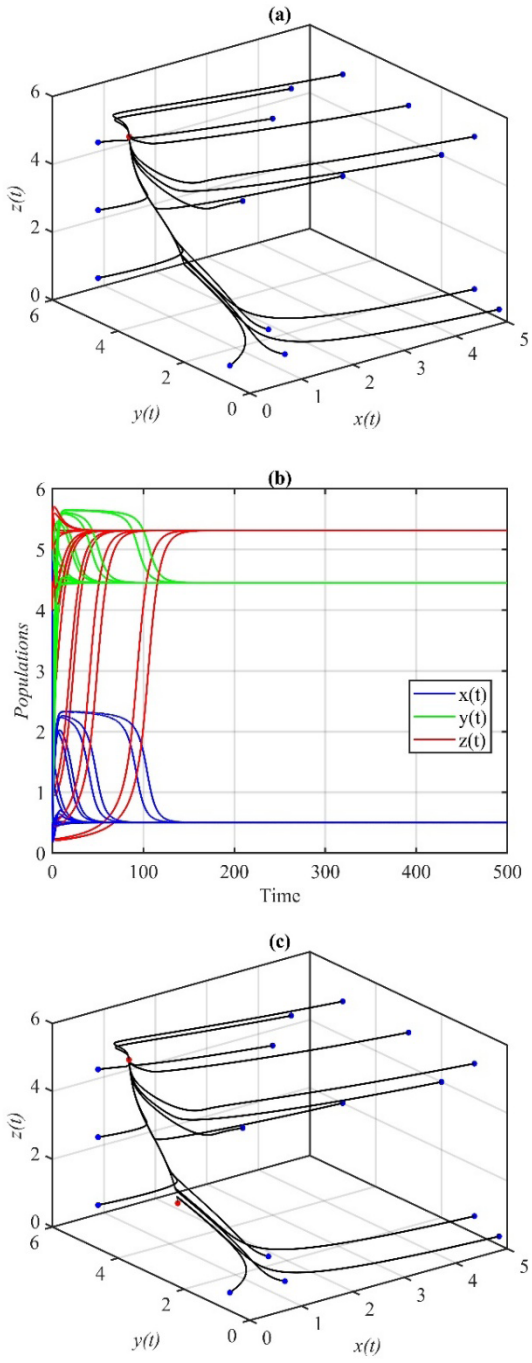


Figure 2. The numerical solutions of **Equation 1** utilizing **Equation 45** and various positive initial points. (a) Three-dimensional (3D) phase plot approaches $E_2 = (0.5, 4.45, 5.31)$ when $= 0.75$. (b) Two-dimensional long-term behavior of populations when $= 0.75$. (c) 3D phase plot shows bistable behavior between $E_1 = (2.14, 5.54, 0)$ and $E_2 = (0.49, 4.44, 5.43)$ when $r = 1$.

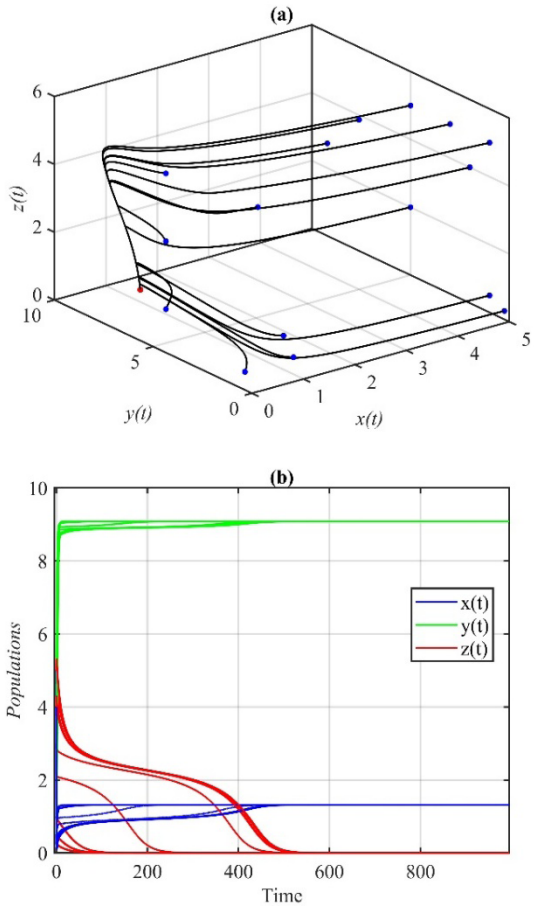


Figure 3. The numerical solutions of **Equation 1** utilizing **Equation 45** and various positive initial points. (a) Three-dimensional phase plot approaches $E_1 = (1.31, 9.09, 0)$ when $\sigma_2 = 0.15$. (b) Two-dimensional long-term behavior of populations when $\sigma_2 = 0.15$.

Figures 1 and **3** explain that for the range $\sigma_2 < 0.16$, the transferred population from protected to unprotected zones is reduced, which leads to a reduction in the population of prey in the unprotected zone, and that is causing extinction in the predator species. Therefore, the positive equilibrium point disappears, and the solution approaches E_1. Otherwise, **Equation 1** undergoes bistability behavior.

Now, altering the parameter β_1 in the ranges $\beta_1 \le 0.26$ and $\beta_1 > 0.26$ makes **Equation 1** approach bistability between E_1 and E_2, and E_2, respectively (**Figures 1** and **4**).

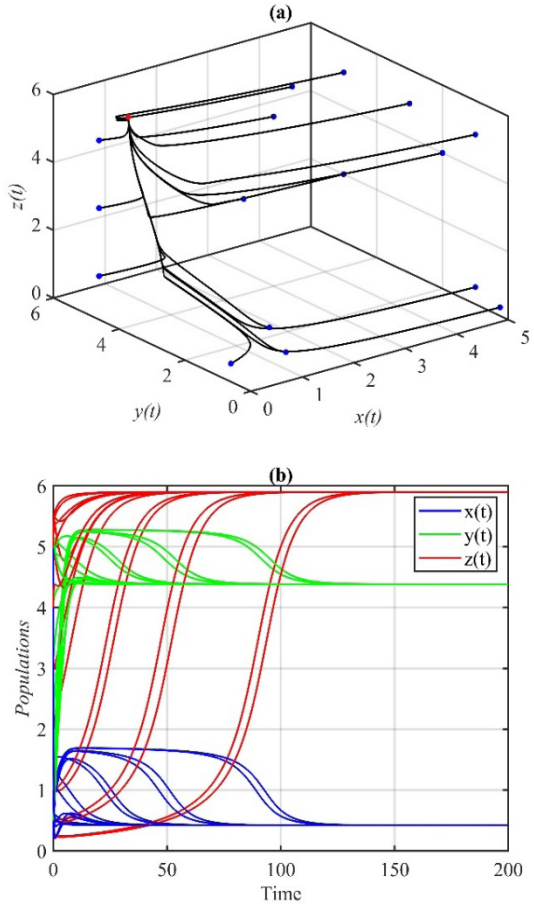


Figure 4. The numerical solutions of **Equation 1** utilizing **Equation 45** and various positive initial points. (a) Three-dimensional phase plot approaches $E_2 = (0.42, 4.38, 5.9)$ when $\beta_1 = 0.3$. (b) Two-dimensional long-term behavior of populations when $\beta_1 = 0.3$.

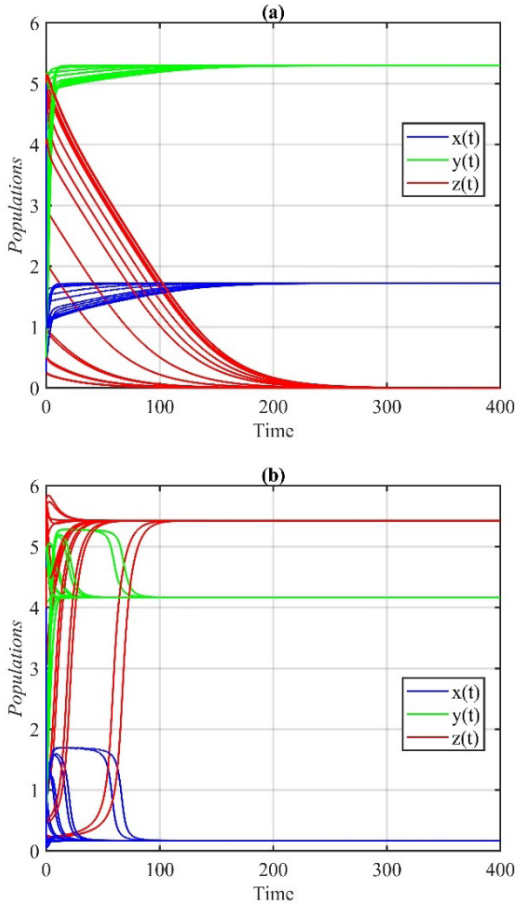


Figure 5. The numerical solutions of **Equation 1** utilizing **Equation 45** and various positive initial points. (a) Two-dimensional (2D) long-term behavior when $\gamma = 0.04$ in which the solutions approach $E_1 = (1.72, 5.3, 0)$. (b) 2D long-term behavior when $\gamma = 0.5$ in which the solutions approach $E_2 = (0.17, 4.16, 5.42)$.

It is clear from **Figures 1** and **4** that if $\beta_1 > 0.26$, then **Equation 21** fails to be satisfied, and hence E_1 becomes an unstable point, which leads to stabilizing **Equation 1** at E_2. This indicates that, for high values of the attack rate coefficient of the predator species, under the same environmental circumstances, an ecosystem can live at a positive stable state.

Moreover, altering the parameter γ in the ranges $\gamma \le 0.05$, $0.05 < \gamma < 0.44$, and $\gamma \ge 0.44$ makes **Equation 1** approach E_1, a bistability between E_1 and E_2, and E_2, respectively (**Figures 1** and **5**).

Figures 1 and **5** explain that if $\gamma \le 0.05$, then E_2 disappears due to the extinction of z, and **Equation 1** approaches E_1. If $\gamma \ge 0.44$, then E_1 becomes unstable, and the basin of attraction of E_2 is extended to include all the interior domain except those multiple unstable positive equilibrium points. Otherwise, the solutions of **Equation 1**exhibit bistability behavior. A dynamic behavior similar to what happens with the change of the γ parameter is observed when changing the parameters $s, l,$ and e. This indicates that, for high values of the cooperative hunting coefficient, under the same environmental

circumstances, an ecosystem can live at a positive stable state.

Finally, altering the parameter β_0 in the ranges $\beta_0 \le 0.07$, $0.07 < \beta_0 \le 0.14$, and $\beta_0 > 0.14$ makes **Equation 1** approach E_2, a bistability between E_1 and E_2, and E_1, respectively (**Figures 1** and **6**).

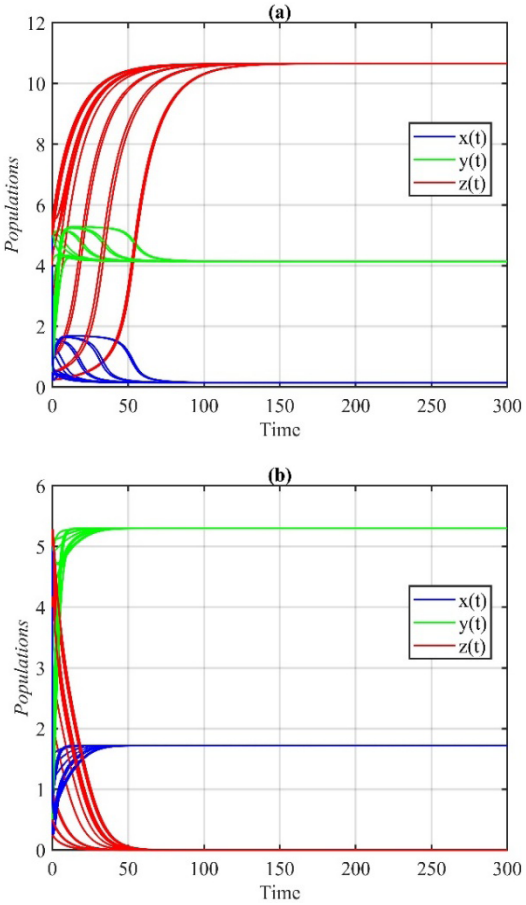


Figure 6. The numerical solutions of **Equation 1** utilizing **Equation 45** and various positive initial points. (a) Two-dimensional (2D) long-term behavior when $\beta_0 = 0.05$ in which the solutions approach $E_2 = (0.13, 4.13, 10.65)$. (b) 2D long-term behavior when $\beta_0 = 0.2$ in which the solutions approach $E_1 = (1.72, 5.3, 0)$.

Figures 1 and 6 explain that if $\beta_0 \le 0.07$, then E_1 becomes unstable, and the basin of attraction of E_2 is extended to include the entire interior domain except for the multiple unstable positive equilibrium points. If $\beta_0 > 0.14$, then E_2 disappears due to the extinction of z, and **Equation 1** approaches E_1. Otherwise, the solutions of **Equation 1** exhibit bistability behavior. This indicates that, for low values of the death rate coefficient of the predator species, under the same environmental circumstances, an ecosystem can live at a positive stable state.

7. Conclusion

In this study, an ecological model was proposed that simulates the prey and predator system when there is an unprotected area where the prey lives and where the predator can prey on it, especially when the predators cooperate when hunting, and a protected area where the prey resorts to shelter from predators, where the predator is unable to enter that area. We have studied the stability and bifurcations of the proposed ecosystem, as well as studied and found the conditions for the persistence of the system. It was noted through the analysis that the system contains at most two boundary equilibrium points, while the positive equilibrium point, if it exists, is multiple.

On the other hand, a numerical study for **Equation 1** using **Equation 45** with different positive initial points shows that although the system has only point attractors, it has a wide range of bistability behaviors. Moreover, it is observed that lowering the prey's growth rate for the unprotected zone or the death rate coefficient of the predator species below a certain value stabilizes **Equation 1** at the $\mathcal{PSEP}$ and guarantees persistence. However, raising the attack rate coefficient of the predator, the cooperative hunting coefficient, the prey's growth rate for the protected zone, carrying capacities of the unprotected zone, or the conversion rate above a certain value stabilizes **Equation 1** at the $\mathcal{PSEP}$ and guarantees persistence. In addition, lowering the prey's migration rate from protected to unprotected zones loses persistence and makes the system stable at $\mathcal{PDFEP}$.

Acknowledgments

None.

Funding

None.

Conflict of interest

The authors declare they have no competing interests.

Author contributions

Conceptualization: All authors
Investigation: All authors
Methodology: All authors
Writing-original draft: Mustafa M. Subhi
Writing-review & editing: Raid Kamel Naji

Availability of data

In this study, we used a hypothetical set of data, which is biologically feasible. Data can be made available to readers by reasonable request to the corresponding author.

AI tools statement

All authors confirm that no AI tools were used in the preparation of this manuscript.

References

1. Lotka, A. J. Elements of physical biology. Williams & Wilkins, Baltimore; 1925.
2. Volterra V. Fluctuations in the abundance of a species considered mathematically. *Nature*. 1926;118(2972):558-560. https://doi.org/10.1038/118558a0
3. Hering RH. Oscillations in Lotka-Volterra systems of chemical reactions. *J Math Chem*. 1990;5(2):197-202. https://doi.org/10.1007/BF01166429
4. Busse FH. Transition to turbulence via the statistical limit cycle route. In H. Haken (Ed.), *Chaos and Order in Nature* (pp. 36–44). Springer-Verlag. 1981. https://doi.org/10.1007/978-3-642-68304-6_4
5. Laval G, Pellat R. Plasma Physics. In Proceedings of the Summer School of Theoretical Physics; Gordon and Breach: New York, NY, USA. 1975.
6. Akhtar P, Karmakar S, Sahoo D, Samanta G. Dynamical analysis of a prey-predator model in toxic habitat with weak Allee effect and additional food. *Int J Dynam Control*. 2024;12(11):3963-3986. https://doi.org/10.1007/s40435-024-01473-w
7. Shao Y, Yu H, Jin C, Fang J, Zhao M. Dynamics analysis of a predator-prey model with Allee effect and harvesting effort. *era*. 2024;32(10):5682-5716. https://doi.org/10.3934/era.2024263
8. Vishwakarma K, Yadav R. Dynamics of a prey-predator model with a strong Allee effect and Holling type-III ratio-dependent functional response. *J Anal*. 2025;33(3):1397-1413. https://doi.org/10.1007/s41478-024-00877-3
9. Alebraheem J, Ibrahim TQ, Arif GE, Hamdi AA, Bazighifan O, Ali AH. The stabilizing effect of small prey immigration on competitive predator-prey dynamics. *Math Comput Model Dyn Syst*. 2024;30(1):605-625. https://doi.org/10.1080/13873954.2024.2366337
10. Diz-Pita É. Global dynamics of a predator-prey system with immigration in both species. *era*. 2024;32(2):762-778. https://doi.org/10.3934/era.2024036
11. Sugié J. Global stabilization and regulation of prey immigration for predator-prey models. *Nonlinear Anal Real World Appl*. 2026;88:104468. https://doi.org/10.1016/j.nonrwa.2025.104468
12. Chen H, Liu M, Xu X. Dynamics of a Prey-Predator Model with Group Defense for Prey, Cooperative Hunting for Predator, and Lévy Jump. *Axioms*. 2023;12(9):878. https://doi.org/10.3390/axioms12090878
13. Roy J, Dey S, Kooi BW, Banerjee M. Prey group defense and hunting cooperation among generalist predators induce complex dynamics: A mathematical study. *J Math Biol*. 2024;89(2):22. https://doi.org/10.1007/s00285-024-02121-9
14. Zhang J, Zhang W. Dynamics of a predator-prey model with hunting cooperation and Allee effects in predators. *Int J Bifurc Chaos*. 2020;30(14):2050199. https://doi.org/10.1142/S0218127420501990
15. Cong P, Fan M, Zou X. Dynamics of a three-species food chain model with fear effect. Commun. *Nonlinear Sci Numer Simul*. 2021;99:105809. https://doi.org/10.1016/j.cnsns.2021.105809
16. Al-Momen SM, Naji RK. The dynamics of modified Leslie-Gower predator-prey model under the influence of nonlinear harvesting and fear effect. *Iraqi J Sci*. 2022;63(1):259-282. https://doi.org/10.24996/ijs.2022.63.1.27
17. Yaseen RM, Helal MM, Dehingia K, Mohsen AA. Effect of the Fear Factor and Prey Refuge in an Asymmetric Predator-Prey Model. *Braz J Phys*. 2024;54(6). https://doi.org/10.1007/s13538-024-01594-9
18. Rayungsari M, Suryanto A, Kusumawinahyu WM, Darti I. Dynamics analysis of a predator-prey fractional-order model incorporating predator cannibalism and refuge. *Front Appl Math Stat*. 2023;9. https://doi.org/10.3389/fams.2023.1122330
19. Uddin MdJ, Khan MdM, Alsulami IM, Shah NA. Ecological Dynamics of a Predator-Prey Model with Cannibalism, Refuge, and Fear: A Bifurcation and Chaos Control Perspective. *Qual Theory Dyn Syst*. 2025;24(5). https://doi.org/10.1007/s12346-025-01370-3
20. Zhang H, Muhammadhaji A. Dynamics of a Delayed Fractional-Order Predator-Prey Model with Cannibalism and Disease in Prey. *Fractal Fract*. 2024;8(6):333. https://doi.org/10.3390/fractalfract8060333
21. Panja P, Gayen S, Kar T, Jana DK. Complex dynamics of a three species predator-prey model with two nonlinearly competing species. *Results Control Optim*. 2022;8:100153. https://doi.org/10.1016/j.rico.2022.100153

22. Ali RA, Ibrahim HA. Effect of wind and disease on the dynamical behavior of a prey-predator system. *Commun. Math Biol Neurosci.* 2025;2025(1):84. https://doi.org/10.28919/cmbn/9305
23. Kebedow KG, Cheru SL, Ega TT. Optimal control strategies in a diseased prey-predator model with Holling type-II dynamics. *J Appl Math.* 2025;2025(1):5535536. https://doi.org/10.1155/jama/5535536
24. Almuallem NA, Mollah H, Sarwardi S. A study of a prey-predator model with disease in predator including gestation delay, treatment and linear harvesting of predator species. *MATH.* 2025;10(6):14657-14698. https://doi.org/10.3934/math.2025660
25. Du Y, Niu B, Wei J. A predator-prey model with cooperative hunting in the predator and group defense in the prey. *DCDS-B.* 2022;27(10):5845. https://doi.org/10.3934/dcdsb.2021298
26. Chen M, Yang W. Role of Cooperative Hunting among Predators and Predator-Dependent Prey Refuge Behavior in a Predator-Prey Model. *J Nonlinear Model Anal.* 2025;7(1):209-228. https://doi.org/10.12150/jnma.2025.209
27. Alani AA, Naji RK. The role of prey vigilance, cannibalism, and hunting cooperation on prey-predator dynamics. *Commun Math Biol Neurosci.* 2025;2025:112. https://doi.org/10.28919/cmbn/9513
28. Umrao AK, Srivastava PK. Impact of hunting cooperation and fear effect in a generalist predator-prey model. *J Biol Syst.* 2024;32(04):1261-1288. https://doi.org/10.1142/S021833902340003X
29. Sahi AM, Satar HA. The Role of the Fear, Hunting Cooperation, and Anti-Predator Behavior in the Prey-Predator Model Having Disease in Predator. *Commun Math Biol Neurosci.* 2024;2024:75. https://doi.org/10.28919/cmbn/8663
30. Ibrahim LR, Bahlool DK. Exploring the Role of Hunting Cooperation and Fear in a Prey-Predator Model with Two Age Stages. *Malays J Math Sci.* 2024;18(4):727-743. https://doi.org/10.47836/mjms.18.4.03
31. Ripple WJ, Larsen EJ. Historic aspen recruitment, elk, and wolves in northern Yellowstone National Park, USA. *Biol Conserv.* 2000;95(3):361-370. https://doi.org/10.1016/S0006-3207(00)00014-8
32. Dubey B. A prey-predator model with a reserved area. *Nonlinear Anal: Model Control.* 2007;12(4):479-494. https://doi.org/10.15388/NA.2007.12.4.14679
33. Huo HF, Jiang HM, Meng XY. A dynamic model for fishery resource with reserve area and taxation. *J Appl Math.* 2012;2012(1):794719. https://doi.org/10.1155/2012/794719
34. Naji RK, Jawad SR. The dynamics of prey-predator model with a reserved zone. *World J Model Simul.* 2016;12(3):175-188. https://www.wjms.org.uk/journal/1746-7233WJMS/wjmsvol12no03paper02.pdf
35. Jawad SR, Naji RK. Stability Analysis of Stage Structure Prey-Predator Model with a Partially Dependent Predator and Prey Refuge. *Int J Eng Manuf.* 2022;12(1):1-11. https://doi.org/10.5815/ijem.2022.01.01
36. Murthy MR, Bahlool DK. A prey-partially dependent predator with a reserved zone: modelling and analysis. *Int J Appl Math Res.* 2016;5(1):1-10. https://doi.org/10.14419/ijamr.v5i1.5238
37. Agnihotri K, Nayyer S. Stability analysis of a predator (bird) - prey (fish) harvesting model in the reserved and unreserved area. *Malaya J Mat.* 2018;6(3):678-684. https://doi.org/10.26637/MJM0603/0032
38. Louartassi Y, Alla A, Hattaf K, Nabil, A. Dynamics of a predator-prey model with harvesting and reserve area for prey in the presence of competition and toxicity. *J Appl Math Comput.* 2019;59(1):305-321. https://doi.org/10.1007/s12190-018-1181-0
39. Rhiati N, Zine R, Louartassi Y. Harvesting of a predator-prey model with two effort functions and Holling type IV response function. *Commun Math Biol Neurosci.* 2025;2025:106. https://doi.org/10.28919/cmbn/9425
40. Chen F. On a nonlinear nonautonomous predator-prey model with diffusion and distributed delay. *J Comput Appl Math.* 2005;180(1):33-49. https://doi.org/10.1016/j.cam.2004.10.001
41. Perko, L., *Differential Equations and Dynamical Systems*, Springer, New York. 2013. https://doi.org/10.1007/978-1-4613-0003-8
42. Freedman HI, Waltman P. Persistence in models of three interacting predator-prey populations. *Math Biosci.* 1984;68(2):213-231. https://doi.org/10.1016/0025-5564(84)90032-4

Mustafa M. Subhi *is an Assistant Lecturer at the Ministry of Education, Russafa 1, Baghdad, Iraq. He received his M.Sc. degree in Mathematics and Computer Applications, College of Science, Al-Nahrain University in 2012. Now, he is a PHD research student in Applied Mathematics, College of Science, University of Baghdad.*
https://orcid.org/0009-0006-4074-5068

Raid K. Naji *has a PhD in Mathematics from IIT-Roorkee, India, in 2003. Currently, he is a full professor in applied mathematics/dynamical systems at the University of Baghdad.*
https://orcid.org/0000-0003-1063-9775



This work is licensed under a Creative Commons Attribution 4.0 International License. The authors retain ownership of the copyright for their article, but they allow anyone to download, reuse, reprint, modify, distribute, and/or copy articles in IJOCTA, so long as the original authors and source are credited. To see the complete license contents, please visit http://creativecommons.org/licenses/by/4.0/.